High-Performance Plastic Platinized Counter Electrode *via* Photoplatinization Technique for Flexible Dye-Sensitized Solar Cells

Nian-Qing Fu,[†,‡] Yan-Yan Fang,[†,‡] Yan-Dong Duan,[†,‡] Xiao-Wen Zhou,[†] Xu-Rui Xiao,[†] and Yuan Lin*[,†]

[†]Beijing National Laboratory for Molecular Sciences, Key Laboratory of Photochemistry, Institute of Chemistry, Chinese Academy of Sciences, Beijing 100190, China and [‡]Graduate School of Chinese Academy of Sciences, Beijing 100039, China

ABSTRACT A photoplatinization technique was proposed to deposit Pt on a thin TiO_2 layer modified indium tin oxide-coated polyethylene naphthalate (ITO/PEN) substrate at low temperature (about 50 °C after 1 h of UV irradiation) for the first time. The fabrication process includes coating and hydrolyzing the tetra-*n*-butyl titanate to form a TiO_2-modified layer and the photoplatinization of the modified substrate in H_2PtCl_6/2-propanol precursor solution under UV irradiation. The obtained platinized electrodes were used as counter electrodes (CE) for flexible dye-sensitized solar cells (FDSCs). The well-optimized platinized electrode showed high optical transmittance, up to 76.5% between 400 and 800 nm (T_{av}), and the charge transfer resistance (R_{ct}) was as low as 0.66 Ω cm^2. A series of characterizations also demonstrated the outstanding chemical/electrochemical durability and mechanical stability of the platinized electrode. The FDSCs with TiO_2/Ti photoanodes and the obtained CEs achieved a power conversion efficiency (PCE) up to 8.12% under rear-side irradiation (AM 1.5 illumination, 100 mW cm^{-2}). The obtained CEs were also employed in all-plastic bifacial DSCs. When irradiated from the rear side, the bifacial FDSC yielded a PCE of 6.26%, which approached 90% that of front-side irradiation (6.97%). Our study revealed that, apart from serving as a functional layer for deposition of Pt, the thin TiO_2 layer modification on ITO/PEN substrates also played an important role in improving the transparency and the mechanical properties of the CE. The effect of the thickness of the TiO_2 layer for Pt coating on the performance of the CE was also investigated.

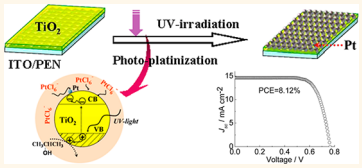

KEYWORDS: flexible dye-sensitized solar cell · platinized electrodes · photoplatinization · optical transparency · electrocatalytic activity

As a promising device for low-cost, environmentally friendly, and large-scale solar energy conversion, dye-sensitized solar cells (DSCs) have been attracting extensive interest,[1−8] and high power conversion efficiency (PCE) over 12% has been achieved.[2] Fabricating DSCs with high efficiency and making the DSC systems more practical for commercial application are new challenges in the development of DSCs. Flexible dye-sensitized solar cells (FDSCs), with significant advantages of device flexibility, light weight, low production cost, suitability for roll-to-roll processes, and broadened utilization field, have been developed and considered as a breakthrough in the commercial application of the DSC system.[4−9] Usually, metal sheets and conducting plastic substrates, such as indium tin oxide (ITO)-coated polyethylene (ITO/PET) and polyethylene naphthalate (ITO/PEN), are employed to replace the rigid transparent conductive oxide (TCO) glass as substrates to fabricate either photoanodes or counter electrodes (CEs) for FDSCs. However, one of the problems with the plastic substrates is that they cannot withstand high-temperature sintering because of the thermolabile nature of this kind of substrate. Therefore, the low-temperature fabrication process becomes the key issue.

In a DSC, the CE takes charge of transferring electrons arriving from the external circuit back to the redox electrolyte and catalyzing the transformation of the triiodide (I_3^-) to iodide (I^-). Until now, platinum has proved the most preferred materials for CE by virtue of its excellent electrocatalytic activity and conductivity with a thickness of only a few nanometers.[10] Although many alternative materials, such as carbonaceous materials,[11−14] conductive polymers,[15,16] and metal compounds,[17−19] have been proposed as catalysts for CEs in DSCs, those materials usually require thick films of around 10 micrometers to achieve a comparable activity to platinum, which makes the CE nontransparent to visible light and also causes the mechanical problems. A transparent CE is essential for the operation of some special

* Address corresponding to linyuan@iccas.ac.cn.

Received for review July 2, 2012 and accepted October 7, 2012.

Published online October 08, 2012
10.1021/nn302944b

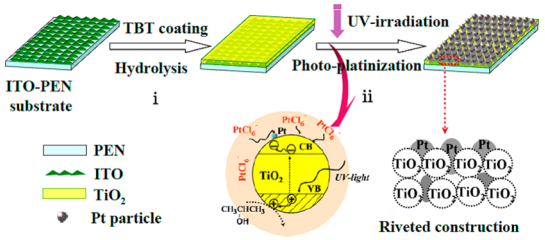

Scheme 1. Schematic flow diagram and mechanism for preparation of platinized electrodes *via* a photoplatinization process: (i) modification of ITO/PEN substrate by a thin TiO_2 layer formed by *in situ* hydrolysis of TBT and (ii) deposition of Pt on modified plastic substrates through a photoplatinization process in H_2PtCl_6/2-propanol precursor solution under UV irradiation.

DSCs such as the FDSCs requiring rear-side irradiation,[5−7] bifacial DSCs,[16,20,21] and DSCs for certain practical applications, such as roof panels and windows or various decorative installations.[22,23] Furthermore, for FDSCs, shape wrenching is unavoidable during handling, transportation, or daily use, so poor adhesion of Pt onto the substrate will result in detaching of Pt from the substrate, leading to detrimental effects on overall solar cell performance and long-term stability.[10,24,25] Therefore, excellent mechanical rigidity (adhesive strength) and stability of the CE against abrasion or general mechanical contact are essential requirements of CEs for flexible devices. So far, sputtering is the most popular technique adopted to fabricate plastic platinized electrodes at low temperature.[26] However, this technique requires relatively harsh production conditions and results in high Pt loading, which increases the production cost. Chemical reduction,[27,28] electrodeposition,[6,29] and electrophoretic deposition[30] are techniques that can fabricate platinized electrodes on various conductive substrates at low temperature, but the adhesive strength of Pt onto the substrate remains an unsolved problem. Therefore, finding a simple but cost-effective technique to fabricate flexible platinized electrodes at low temperature meeting all the requirements, including high catalytic activity and conductivity, high transparency, low Pt loading, excellent mechanical stability, and chemical/electrochemical durability, simultaneously is still a demanding, imperative task.

Photoplatinization is a wonderful technology developed to prepare a platinum-loaded TiO_2 particle suspension or TiO_2 film for photocatalytic degradation.[31−33] However, to the best of our knowledge, scarcely any work had been reported to adopt this technique for depositing Pt on conductive substrates as CEs for DSCs. Herein, we report for the first time that high-performance plastic platinized electrodes can be fabricated on TiO_2 thin layer decorated ITO/PEN substrates through a modified photoplatinization technique (Scheme 1). This new method is a simple and cost-effective process that can be carried out at low temperature. The obtained platinized electrode shows high optical transmittance, low R_{ct}, and excellent mechanical as well as chemical/electrochemical stability. Its properties and applications in rear-side-irradiated FDSCs and bifacial FDSCs have been investigated by systematic measurements.

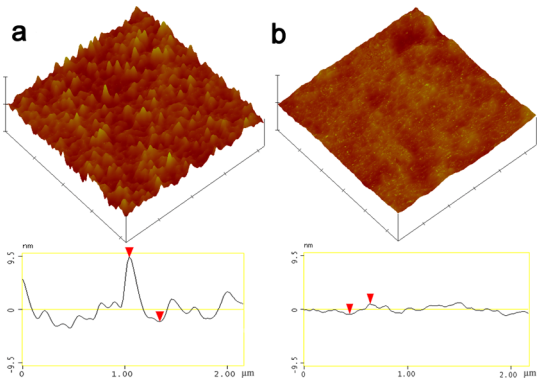

Figure 1. AFM morphology and cross-sectional profiles of (a) blank ITO/PEN surface and (b) TiO_2-modified ITO/PEN surface.

RESULTS AND DISCUSSION

Preparation of the Plastic Platinized Electrode. The plastic platinized electrodes were fabricated on the ITO/PEN substrate *via* a photoplatinization technique. The overall strategies of the process are illustrated in Scheme 1, involving the step of modification of the ITO/PEN substrate with a TiO_2 thin layer and the following deposition of Pt on the modified substrate *via* a photoreduction process in H_2PtCl_6/2-propanol precursor solution under UV irradiation. In the first step, a transparently smooth TiO_2 layer was formed *in situ* on the ITO surface from the tetra-*n*-butyl titanate (TBT) through spin-coating followed by hydrolysis in distilled water at 100 °C. As shown in the AFM images of Figure 1, the root-mean-square (rms) roughness of the ITO surface dramatically decreases from 3.6 to 0.47 nm after the TiO_2 (25 nm in thickness) modification. The SEM images of Figure S1 (Supporting Information) also reveal that the scalelike grain boundary of the ITO surface is successfully leveled by the smooth TiO_2 film and no TiO_2 particles with a size larger than 5 nm can be observed on the modified surface. The TiO_2 prepared by the hydrolysis process has been confirmed to be anatase by our previous work and by Lee as well.[34,35] In the second step, the treated substrate was immersed in the H_2PtCl_6/2-propanol precursor solution and exposed to UV irradiation. Under UV irradiation, electron−hole couples are generated in the thin TiO_2 film according to reaction 1 and then transferred to the TiO_2 surface independently. The photogenerated electrons increase on the surface of TiO_2 while the holes are captured by the hole scavenger (here this means 2-propanol) according to reaction 2. Then, the Pt ions ($PtCl_6^{2-}$) adsorbed on the TiO_2 surface are

reduced to neutral Pt by the photogenerated electrons according to reactions 3 and 4.

$$TiO_2 + h\nu \rightarrow TiO_2(e\cdots h) \rightarrow TiO_2(e^- + h^+) \quad (1)$$

$$(CH_3)_2CHOH + h^+ \rightarrow {}^{\bullet}(CH_3)_2CHO + H^+ \quad (2)$$

$$Pt^{IV}Cl_6^{2-} + 2e^- \rightarrow Pt^{II}Cl_4^{2-} + 2Cl^- \quad (3)$$

$$Pt^{II}Cl_4^{2-} + 2e^- \rightarrow Pt^0 + 4Cl^- \quad (4)$$

The key step for successful preparation of the platinized electrode is the modification of the substrate with TiO_2, which makes the deposition of Pt possible. The digital photograph in Figure 2a demonstrates clearly that, after the photoplatinization process, the modified ITO/PEN substrate became slightly dark (right side), suggesting the growth of Pt on the substrate, while no significant color change was observed for the bare substrate (left side). This is because, unlike TiO_2, the indium tin oxide (band gap of the ITO is between 3.5 and 4.3 eV[36]) is hardly excited by the UV light used in our experiment (350−450 nm, essentially emitting at 365 nm); thereby, the photogenerated electrons, which are responsible for the reduction of Pt ions to Pt^0, cannot be formed. As a result, Pt ions cannot be reduced and the Pt cannot grow on the bare ITO/PEN substrate. Additionally, the adsorption of noble metal precursor ions on the surface (*i.e.*, TiO_2 surface) is regarded as an indispensable step before they can be reduced by the photogenerated electrons. It is well known that TiO_2 in alcoholic solution is usually positively charged, which is more attractive for the adsorption of the $PtCl_6^-$ anions. As a result, the photoreduction of Pt ions on the TiO_2 surface is more facilitated. The X-ray photoelectron spectroscopy (XPS) analysis revealed that the Pt deposited on the electrode was Pt(0), as shown in Figure S2.

Surface and Morphology Characterization of the Platinized Electrodes. The scanning electron microscopy (SEM) and transmission electron microscopy (TEM) images in Figure 2b−d show the typical surface morphology of CE0.13 (see details in the Experimental Section). Figure 2b depicts two morphologies of Pt on the electrode surface: the Pt aggregates of around 100 nm and small Pt particles with a size of about 5 nm. The morphology of Pt is further confirmed by TEM measurements. Figure 2c demonstrates the existence of Pt aggregates and small Pt particles, and Figure 2d reveals that the Pt aggregate is the coagulation of small granules with diameters of about 3−5 nm, and many pores are formed in the aggregate due to the packaging of the small granules. The lattice spacing of the Pt shown in Figure 2d is 0.23 nm, which is consistent with the most catalytically active spacing of the Pt(1 1 1) plane.[37] The reduction-active center induced growth mechanism will account for the

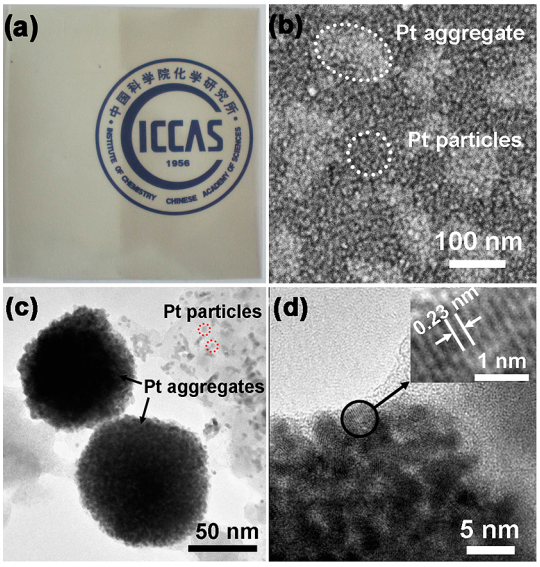

Figure 2. (a) Digital photograph comparing the photoplatinized ITO/PEN substrate with (right) or without (left) TiO_2 modification. (b) SEM image of the platinized electrode (CE0.13) derived from the photoplatinization technique. (c, d) TEM and HRTEM images of the Pt aggregates and Pt particles from CE0.13, respectively.

formation of the Pt aggregates. It is reasonable that there are some defect states on the surface of the TiO_2 film. During the UV irradiation, the defect states will trap more photogenerated electrons than other parts; therefore, some reduction-active centers are formed and those active centers are more competitive for the reduction of $PtCl_6^{2-}$ and $PtCl_4^{2-}$. As a result, Pt grows more quickly on those centers and Pt aggregates are formed. The tailored structure of the Pt aggregates will further render the electrode with high surface area, which is favorable for good catalytic activity. However, the existence of the Pt aggregates on the electrodes will also decrease the transparency of the electrode and increase the Pt loading as well. Methods that can quench the reduction-active centers and suppress the growth of the Pt aggregates will be useful to fabricate platinized electrodes with a more homogeneous Pt dispersion.

Transparent Property of the CEs. The optical transparency of the CE is essential for the bifacial DSC or the device requiring rear-side irradiation. Figure 3 shows the optical transmittance spectra of CE0.13. The obtained platinized electrode shows a high transparency, ranging from 450 to 800 nm with a T_{av} between 400 and 800 nm of 76.5%, revealing that, compared with the blank substrate (T_{av}, 79.1%), only less than 3% of the transmittance is lost after the Pt deposition. Interestingly, Figure 3 also demonstrates that the transparency of the ITO/PEN substrate, especially in the short-wavelength range, has been improved after TiO_2 modification. The T_{av} increases from 79.1% to 82.5% after the substrate was modified by a thin TiO_2 film. It is well known that light of shorter wavelength is relatively

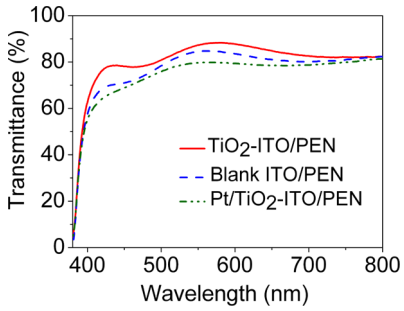

Figure 3. Optical transmittance of ITO/PEN, TiO_2-modified ITO/PEN (TiO_2—ITO/PEN), and Pt/TiO_2—ITO/PEN (CE0.13).

more easily scattered on a rough surface than that of a longer wavelength, since the scattering efficiency of light is proportional to $1/\lambda^4$, where λ is the wavelength of incident light.[38] Figure 1and Figure S1 demonstrate that the scalelike grain boundary of ITO was leveled by the smooth TiO_2 layer. Obviously, this enhancement of transparency can be attributed to the improved surface uniformity of the modified surface.[38,39] The antireflection effect will contribute additionally to the transparency of the CEs and then improve the performance of the DSCs with rear-side irradiation or the bifacial DSCs.

Electrocatalytic Activity of the CEs. The charge transfer resistance (R_{ct}) at the platinized electrode/electrolyte interface was investigated by electrochemical impedance spectroscopy (EIS) measurements, which were performed on the DSCs under AM 1.5 illumination in open-circuit voltage conditions. The equivalent circuit of this type of cells is described in the inset of Figure 4a, which includes the series resistance (R_s) in the high-frequency region. The RC processes of the platinized electrode/electrolyte interface consist of interfacial charge transfer resistance (R_{ct}) and capacitance of the electrical double layer (CPE1) in the medium-frequency region, and the RC processes of the TiO_2 electrode/electrolyte interface consist of interfacial charge transfer resistance (R_R) and capacitance of the depletion layer of the TiO_2 electrode (CPE2) in the low-frequency region. The electrocatalytic performance of the platinized electrode toward triiodide reduction can be evaluated in terms of R_{ct}, which is determined by the diameter of the semicircle presented in the medium-frequency region of impedance spectra.[6] Figure 4a presents the Nyquist plots of the DSCs employing CEs prepared by photoplatinization, thermal decomposition, and electrodeposition, respectively. The R_{ct} of the CE prepared by photoplatinization (CE0.13) is detected to be 0.66 Ω cm^2, which is comparable to that by thermal decomposition (0.59 Ω cm^2) and much better than that by electrodeposition (2.54 Ω cm^2), indicating the superior electrocatalytic activity of the platinized electrode prepared by the photoplatinization technique. To further characterize the properties of the platinized electrodes, the electrical double-layer

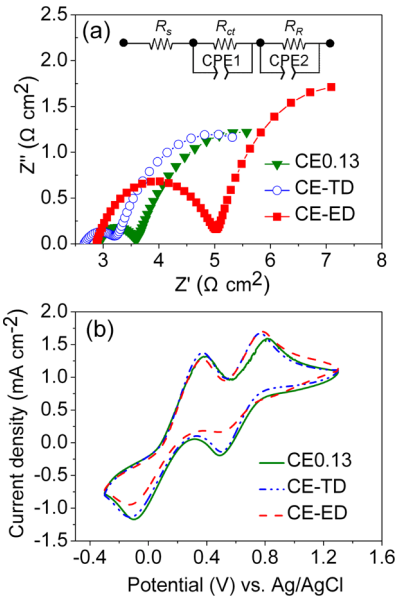

Figure 4. (a) Nyquist plots of the TiO_2/Ti photoanode-based DSCs employing three different CEs, obtained in open circuit conditions. The inset is the equivalent circuit of DSCs. (b) Cyclic voltammograms of the various CEs in acetonnitrile solution containing 10 mM LiI, 1 mM I_2, and 0.1 M $LiClO_4$; scan rate 100 mV s^{-1}. CE0.13, CE-TD, and CE-ED represent the CEs prepared by photoplatinization, thermal decomposition, and electrodeposition, respectively.

capacitance C, which is related to the surface area, was obtained by fitting the Nyquist plots shown in Figure 4a using the following expression, according to our previous work.[6]

$$Z_{CPE1} = C(j\omega)^{-\beta}$$

The values of C are 1412, 1307, and 740 μF cm^{-2} for CEs prepared by photoplatinization (CE0.13), thermal decomposition, and electrodeposition, respectively. Compared to the C value of 10—40 μF cm^{-2} for the typical Pt electrode with ideal flat surface,[40] the surface area of CE0.13 is about 56 times higher than that of a Pt electrode with ideal flat surface (using 25 μF cm^{-2} for the Pt electrode for the calculation). The high catalytic surface area of the CE0.13 arises from (1) the new rough surface of the Pt aggregates and particle layer formed on the nanoporous TiO_2 film surface and (2) the riveted construction of the Pt in the nanoporous TiO_2 film (as shown in Scheme 1). The high surface area will render the CEs with high catalytic activity. To our knowledge, to date, this is the lowest R_{ct} value reported for a flexible platinized electrode fabricated at low temperature with high optical transparency.[6,28,29,41]

To further verify the electrocatalytic activity of the obtained platinized electrodes, cyclic voltammograms recorded between −0.3 and 1.3 V in the electrolyte solution composing of 1 mM I_2, 10 mM LiI, and 0.1 M $LiClO_4$ in acetonitrile at a scan rate of 100 mV s^{-1} are shown in Figure 4b. In Figure 4b, two pairs of redox peaks are observed for all three electrodes. The left

cathodic peak corresponds to the reduction of I_3^- to I^- and is of interest in this research. The CEs prepared by photoplatinization (CE0.13) and thermal decomposition show similar high cathodic peak current density, indicating the high electrocatalytic activity of these two kinds of electrodes. This result is in agreement with the EIS result.

Mechanical and Chemical/Electrochemical Stability of the CEs. Excellent mechanical rigidity and stability of the CE against abrasion or general mechanical contact is a desired property of a CE of a DSC.[10,23] The adhesive strength of the Pt on the substrate was estimated by the adhesive tape test, which was carried out in terms of a scrape peeling under a pressure of 150 psi with the assistance of a screen printing machine (Figure S3). For this test, platinized electrodes were covered by adhesive tape (3M) and fixed on the platform of a screen printing machine (ATMA TUNG YUAN M/C Ind. (Kunshan, China) Co., Ltd.). Then, the scraper of the machine was quickly scraped across the platinized electrode (0.5 m/s) under a pressure of 150 psi. After that, the adhesive tape was peeled of with a speed of 0.5 m/s under the control of the screen printing machine. The treated CEs were used to assemble unsealed FDSCs, and the R_{ct} values were obtained by EIS measurements. After the above measurements, the platinized electrode was washed by ethanol and dried in an 80 °C oven for 10 min before another adhesive tape-scraping process was carried out. Figure 5a shows the R_{ct} values as a function of the times of the adhesive tape tests. It reveals that the R_{ct} of CE0.13 increases slightly after the first adhesive tape peeling and remains almost unchanged for the following three cumulative times, indicating that the Pt aggregates and particles are mechanically very robust against abrasion on the substrate. The mechanical property of the electrode prepared by photoplatinization is as good as that of the electrode prepared by thermal decomposition and much better than the electrodeposited one. SEM images (Figure S4) reveal that there are no significant differences in the surface morphologies of the electrodes prepared by photoplatinization and thermal decomposition, while a large portion of the Pt particles on the electrodeposited electrode are detached after four cumulative adhesive tape peelings. From the mechanism of the photoplatinization process, it can be known that the initial photoreduction of Pt ions to neutral Pt is occurring at the surface of TiO_2, the interfaces of individual TiO_2 crystals, and the inner surface of the micropores in the TiO_2 layer. This makes the Pt particle grow as a tenon by inserting part of its body into the TiO_2 layer to form a riveted construction (Scheme 1), which was confirmed by the graded distribution of Pt element shown in the SEM/EDX mapping photo of Figure S5. Additionally, the thin TiO_2 layer formed on the substrate surface demonstrates excellent adhesion to the ITO/PEN substrate and is very difficult to strip off without damaging the ITO layer. As a result, the thin TiO_2 layer between Pt particles and the ITO substrate acts as a kind of solid glue and makes the substrate and the Pt film well-integrated, leading to the excellent mechanical stability of the platinized electrodes.

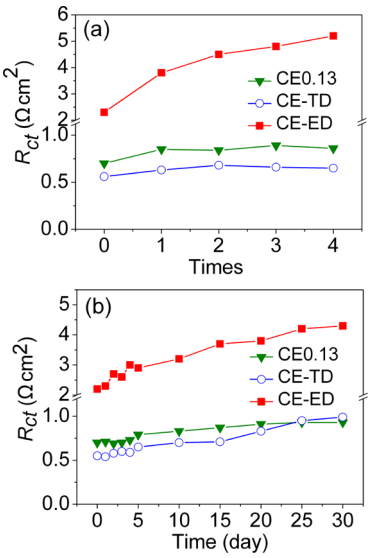

Figure 5. (a) Influence of R_{ct} of DSCs with different CEs on the times of adhesive tape tests applied on the CEs. (b) R_{ct} of DSCs with different CEs over time. CE0.13, CE-TD, and CE-ED represent the CEs prepared by photoplatinization, thermal decomposition, and electrodeposition, respectively.

The chemical/electrochemical durability of the platinized electrodes was evaluated by the time-related EIS measurements. Figure 5b shows that the increase of R_{ct} of the DSC, utilizing the CE0.13 as CE, over time is much less than that of the device employing an electrodeposited CE, and the durability of CE0.13 is even better than that of the electrode prepared by thermal decomposition. The outstanding durability of the as-prepared platinized electrode is, to a great extent, attributed to the good adhesion of the Pt particles onto the substrate, since poor adhesion of the Pt onto the substrate can result in Pt migration, even detaching from the substrate, leading to detrimental effects on overall solar cell performance and long-term stability.[10,23,24]

Photovoltaic Performance of the Flexible DSCs. The $J-V$ curves of the DSCs employing TiO_2/Ti photoanodes and different platinized CEs prepared by photoplatinization, thermal decomposition, and electrodeposition, respectively, measured under AM 1.5 simulated sunlight (100 mW cm^{-2}) are presented in Figure 6a; the resultant photovoltaic parameters are summarized in Table 1. In this study, the performance parameters, namely R_{ct} and transparency, of the platinized CEs were optimized to render DSCs with the best performance. The T_{av} of the platinized CEs prepared by photoplatinization, thermal decomposition, and electrodeposition is 76.5%, 76%, and 72.4%, respectively, as

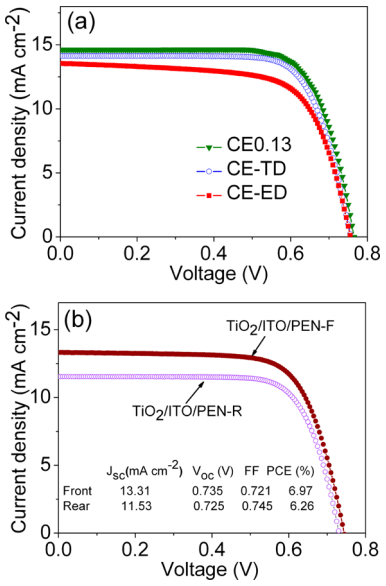

Figure 6. (a) Photocurrent–voltage characteristics of the DSCs employing a TiO_2/Ti photoanode and different platinized CEs prepared by photoplatinization (CE0.13), thermal decomposition (CE-TD), and electrodeposition (CE-ED), respectively. (b) Photocurrent–voltage characteristics of the FDSCs employing a TiO_2/ITO/PEN photoanode and CE0.13 under front- (solid circles) and rear-side (open circles) irradiation measured under AM 1.5 simulated illumination (100 mW/cm^2).

TABLE 1. Photovoltaic Characteristics of DSCs with TiO_2/Ti Photoanodes and Different CEs under Rear-Side Irradiation[a]

CE[b]	T_{av},[c] %	J_{sc},mA/cm^2	V_{oc}, V	FF	PCE, %
CE0.13	76.5	14.63	0.755	0.736	8.12
CE-TD	76	14.25	0.745	0.739	8.03
CE-ED	72.4	13.56	0.75	0.674	6.82

[a] The data in the table are the mean values of five samples, and the data were obtained under AM 1.5 simulated sunlight (100 mW cm^{-2}). The photoactive area is 0.2 cm^2. [b] CEs used here were prepared by photoplatinization (CE0.13), thermal decomposition (CE-TD), and electrodeposition (CE-ED), respectively. [c] Average transmittance between 400 and 800 nm.

shown in Figure S6. The flexible devices employing CE0.13 as CEs give a short-circuit current density (J_{sc}) of 14.63 mA cm^{-2}, an open-circuit voltage (V_{oc}) of 755 mV, and fill factor (FF) of 0.736, leading to a PCE as high as 8.12% in the rear-side irradiation condition. The PCE is even a little higher than that of the DSC based on the CE prepared by thermal decomposition (8.03%) and much better than that of the device with electrodeposited CE (6.82%), owing to both the high electrocatalytic activity and high transparency of the CEs fabricated by the photoplatinization technique. Furthermore, the long-term stability test performed on the DSCs based on CE0.13 also reveals that the PCE of the DSCs based on photoplatinized CEs maintains 93% of its initial values after 30-days storage in an air atmosphere, and the deterioration of both J_{sc} and PCE appears mostly in the first 15 days after the devices were fabricated and sealed (Figure S7).

TABLE 2. Property Parameters of the CEs Obtained with Various $H_2PtCl_6 \cdot 6H_2O$ Concentrations and the Corresponding J–V Characteristics of FDSCs Employing These CEs[a]

CEs	T_{av},[b] %	R_{ct}, Ω cm^2	Pt loading, μg/cm^2	J_{sc},mA/cm^2	V_{oc}, V	FF	PCE, %
CE 0.5	47.6	1.59	10.35	9.10	0.755	0.725	4.95
CE 0.2	67.4	1.48	4.52	13.05	0.745	0.732	7.05
CE 0.13[c]	76.5	0.66	3.95	14.63	0.755	0.736	8.12
CE 0.1	78.8	7.97	2.51	15.05	0.745	0.491	5.49

[a] All data in the table are the mean values of five samples, and the J–V data were obtained under AM 1.5 simulated sunlight (100 mW cm^{-2}). The photoactive area is 0.2 cm^2. [b] Average transmittance between 400 and 800 nm. [c] For a comprehensive comparison, the data of the DSCs employing CE0.13 as CEs are presented in this table again.

The TiO_2 photoanodes were also fabricated on the ITO/PEN plastic substrate to make bifacial FDSCs in combination with the obtained transparent CE0.13. Figure 6b shows the photocurrent–voltage curves of the bifacial FDSCs corresponding to the front- and rear-side irradiation. When irradiated from the rear side, the bifacial FDSC exhibits a PCE of 6.26%, which approaches 90% that of the front-side irradiation (6.97%). The high PCE of the bifacial FDSC under rear-side irradiation is ascribed to the high catalytic activity and high transparency of the CE, which has minimized the energy loss in the rear-side irradiation condition. The J_{sc} of the device is lower for the case of rear-side irradiation than that under the front-side irradiation because the CE and the electrolyte absorb part of the incident light. Owing to the similar series resistance of the device for both cases, the FF under rear-side irradiation is slightly higher than that under front-side irradiation because lower J_{sc} values usually provide high FF values.[20] The decrease of V_{oc} can also be attributed to the lower light intensity cast on the dye-sensitized TiO_2 photoanode under rear-side irradiation.[16,42]

Effect of H_2PtCl_6 Concentration in Precursor Solution on Performance of CEs and DSCs. The H_2PtCl_6 concentration in the precursor solution for fabricating platinized electrodes through the photoplatinization technique is a key factor in the performance of CEs and thus the DSCs under rear-side irradiation. The data listed in Table 2 reveal that platinized electrodes derived from a Pt precursor solution with lower H_2PtCl_6 concentration show higher transparency. The T_{av} increases from 47.6% to 78.8% while the applied H_2PtCl_6 concentration decreases from 0.5 mM to 0.1 mM. The SEM and SEM/EDX images, shown in Figure S8, reveal that the electrodes derived from Pt precursor solution with higher H_2PtCl_6 concentration show "thicker" Pt aggregates and a denser distribution of small Pt particles, which are responsible for the decreased transparency. The Pt-loading data also confirm that more Pt is deposited on the electrodes when a precursor solution with higher H_2PtCl_6 concentration is used. Interestingly, it can be seen from Table 2 that the R_{ct} first decreases with the decreasing of the H_2PtCl_6

concentration, reaching the lowest value of 0.66 Ω cm^2 at 0.13 mM, and then increases dramatically to 7.97 Ω cm^2 at a H_2PtCl_6 concentration of 0.1 mM. We assume that, in the case of high H_2PtCl_6 concentration preparation, the excess Pt particles overlapped on the already located Pt particles have a less positive impact on increasing the active surface and jam and enclose the pores in the Pt film, which hinders the diffusion and penetration of the I_3^-. As a result, the catalytic activity of the platinized electrodes deteriorates. This tendency is in accordance with the reported work.[24] The properties of the CEs, namely, transparency and electrocatalytic activity, have a direct influence on the performance of the DSCs under rear-side irradiation. As demonstrated in Table 2, the J_{sc} of the FDSCs, employing TiO_2/Ti photoanodes and CE0.5, CE0.2, CE0.13, and CE0.1 as CEs, respectively, increases dramatically from 9.10 to 15.05 mA cm^{-2}, while V_{oc} is almost unchanged. On the other hand, all FDSCs with these platinized CEs, except CE0.1, give high FF but a slight increase in the order CE 0.5, CE 0.2, and CE 0.13. For the FDSCs employing CE0.5, CE0.2, and CE0.13 as CEs, the PCE of the devices increases from 4.95% to 8.12%. However, when CE0.1 is used, the positive effect of improved optical transparency on the PCE is offset by the decreased FF, owing to its poor electrocatalytic activity; as a result, the performance of the device deteriorates.

Effect of Thickness of Modified TiO_2 Layer on Performance of CEs and DSCs. The thickness of the modified TiO_2 layer is very essential to achieve CEs with high transparency and conductivity. The TiO_2 thickness is varied from a few nanometers to hundreds of nanometers (*i.e.*, 0, 8, 25, 70, and 560 nm) by altering the TBT concentration in the titanate precursor solution (*i.e.*, 0, 3, 10, 30, and 100 mM). From Table S1, it is clear that the T_{av} of the substrates first increases with increasing TiO_2 thickness, until the highest value of 82.6% at 70 nm was achieved, due to the antireflection effect, then it decreases with a further increase in the TiO_2 thickness, originating from the semitransparent nature of the thick TiO_2 film prepared under high TBT concentration. Meanwhile, the square resistance of the substrates increases consecutively from 18 to 740 Ω/□ and will influence the performance of the CE as well as the DSC. All of the CEs were prepared through the photoplatinization process in 0.13 mM H_2PtCl_6 precursor solution. The detailed parameters of transparency and Pt loading of the CEs are also listed in Table S1, which reveals that the transparency decreases with an increase of the thickness of the TiO_2 film, while the Pt loading increases with an increase of the TiO_2 thickness. The increase of the Pt loading with an increase of the thickness of the TiO_2 film dominates the contribution to the decreased transparency. Meanwhile, it also provides further evidence to the speculation of the riveted construction as mentioned in Scheme 1. Given that the flat surface of the TiO_2 film provides a similar surface area for the surface-loaded Pt in all cases and the surplus of Pt must originate from the ones inserted into the nanopores in the TiO_2 film, a thicker TiO_2 film can afford more pores. The photovoltaic parameters as well as the R_{ct} values of the DSCs using the CEs prepared on the substrates with various TiO_2 thicknesses are summarized in Table S2. It reveals that the R_{ct} first decreases and achieves a lowest value of 0.66 Ω cm^2 when the CE was prepared on the 25 nm TiO_2 film modified substrate. The enhancement of the electrocatalytic activity is attributed to the increased Pt loading on the electrode with a thicker TiO_2 layer. However, a further increase of the thickness decreases the activity of the CEs because the thick TiO_2 layer will increase the square resistance of the CEs, which hinders the transfer of the electrons from the external circuit to the catalytic layer. The J_{sc} of DSCs using the CE with TiO_2 of 8 nm thickness shows the highest value of 15.02 mA cm^{-2} and slightly decreases to 14.63 mA cm^{-2} when the CE with TiO_2 of 25 nm thickness was used, owing to the slight decrease in transparency. The J_{sc} drops significantly when the TiO_2 film is thicker than 70 nm; this can be attributed to the decreasing of the transparency and, especially, the poor electrocatalytic activity of the CEs. The V_{oc} of the DSCs suffers a continual decrease with an increase of the thickness of the TiO_2 layer because the TiO_2 layer will obstruct the transfer of the electrons and promote the back reaction and the recombination. The highest PCE of 8.12% was yielded when the CE was fabricated on the 25 nm TiO_2 film modified substrate; this PCE value is slightly higher than that of the device with its CE prepared on the substrate modified by an 8 nm TiO_2 layer due to the higher FF. From Table S2, it can also be seen that the DSCs with CE prepared on the unmodified substrate also obtain a PCE of 2.28% because the blank substrate can physically absorb some Pt particles formed in the reaction solution. However, the PCE dropped sharply to 0.5% after the adhesive tape test due to the poor adhesion of the physically absorbed Pt particles onto the substrate.

CONCLUSION

In conclusion, we have developed a novel photoplatinization technique to fabricate flexible platinized CE on an ITO/PEN substrate at low temperature for DSCs. The as-prepared electrode has the following merits simultaneously: (1) high catalytic activity and conductivity for fast reduction of triiodide; (2) high transparency for the requirement of rear-side irradiation and bifacial DSCs; (3) excellent mechanical stability against abrasion or general mechanical contact; (4) outstanding chemical/electrochemical durability for long-term service life; (5) low Pt loading (3.5 $\mu g \cdot cm^{-2}$) for acceptable price-to-performance ratio. A high PCE of 8.12% for a flexible DSC employing a TiO_2/Ti

photoanode and the obtained platinized CE was achieved. The flexibly bifacial DSC with a plastic photoanode and the obtained CE exhibited similarly high photovoltaic performance for both front- and rear-side irradiation. The ratio of the PCE under rear- and front-side irradiation (PCE_R/PCE_F) is up to 0.90. Furthermore, the photoplatinization technique presented here can also be used to deposit Pt or other noble metals on various substrates without any shape limitation for DSCs or other devices with special geometrical configurations.

EXPERIMENTAL SECTION

Preparation of Platinized Counter Electrode. The plastic platinized electrodes were fabricated through the photoplatinization technique, which can be divided into two consecutive steps: modification of the ITO/PEN substrate by TiO_2 and the following growth of Pt on the modified substrate *via* photoplatinization. The modification of the substrate was carried out as follows: A tetra-*n*-butyl titanate solution with 10 mM TBT concentration was prepared by adding a certain amount of TBT into a mixture of 2-propanol and *n*-butyl alcohol (v/v = 1:1). The ITO/PEN substrates (84.2% transmittance at 550 nm) were subject to consecutive ultrasonic cleaning in detergent solution, distilled water, and acetone and finally dried by blowing air before using. For TBT coating, TBT solution (150 μL) was spread on the 3 cm $\times$ 3 cm substrate, using adhesive tape as a frame, and rotated at 150 rpm at 70 °C. After that, the treated substrates were immersed in distilled water and kept at 120 °C for 2 h to complete the transformation of TBT to TiO_2, and then the substrates were dried at 100 °C for 30 min to finish the modification and functionalization of substrate by a TiO_2 thin layer. The process of growing Pt particles on the modified substrate was described as below: 0.1 M $H_2PtCl_6 \cdot 6H_2O$ solution was prepared by dissolving a certain amount of $H_2PtCl_6 \cdot 6H_2O$ in 2-propanol. For photoplatinization, a piece of the TiO_2-modified substrate was placed on a sample holder and immersed in 20 mL of Pt precursor solution with a certain concentration prepared by diluting the 0.1 M $H_2PtCl_6 \cdot 6H_2O$ solution with 2-propanol. The TiO_2-modified surface was oriented toward the bottom of the quartz vessel. The reaction system was first stored in dark conditions for 30 min to reach the equilibrated adsorption of $PtCl_6^-$ ions on the surface of TiO_2. Subsequently, the reaction vessel was exposed for about 1 h to UV radiation arising from a high-voltage mercury lamp (300 W; wavelength range: 350−450 nm, essentially emitting at 365 nm) located 15 cm below the reaction vessel. The obtained platinized electrode was rinsed with plenty of deionized water and ethanol several times and then subjected to a heat treatment at 80 °C for 4 h. The platinized electrodes produced with a $H_2PtCl_6 \cdot 6H_2O$ concentration of 0.1, 0.13, 0.2, or 0.5 mM are abbreviated as CE0.1, CE0.13, CE0.2, and CE0.5, respectively. To investigate the effect of the thickness of the TiO_2 layer on the performance of the CEs and DSCs, TBT solutions with various TBT concentrations (*i.e.*, 0, 3, 10, 30, 100 mM) were used to deposit a TiO_2 film with different thicknesses on the substrates, and a 0.13 mM $H_2PtCl_6 \cdot 6H_2O$ precursor solution was used for photoplatinization. For comparison, the platinized FTO glass CEs were prepared by spreading drops of 0.5 mM $H_2PtCl_6 \cdot 6H_2O$/2-propanol solution on the FTO glass (82.1% transmittance at 550 nm) followed by a sintering at 390 °C in air for 15 min. The plastic CEs were also prepared on ITO/PEN substrates by electrodeposition according to the reported work.[28] The CEs prepared by thermal decomposition and electrodeposition are abbreviated CE-TD and CE-ED, respectively.

DSC Fabrication. Before TiO_2 coating, a Ti sheet (0.1 mm thickness) was subjected to treatment in 0.5 M hydrofluoric acid aqueous solution for 2 min and subsequently ultrasonically cleaned in distilled water and acetone, respectively. A viscous TiO_2 paste (particle size: 12 nm) was screen-printed (200 T mesh) on the Ti sheet with three layers, giving films with a thickness of ~16 μm. The printed films were dried in air for 30 min and then sintered at 500 °C for 30 min in air. The plastic photoanodes with 12 μm TiO_2 film were fabricated by coating three layers of TiO_2 paste composed of a mixture of 20 and 100 nm diameter TiO_2 particles with a weight ratio of 7 to 3 on the ITO/PEN substrate followed by a mechanical compression at 100 MPa according to the reported work.[9] The two kinds of TiO_2 electrodes at about 80 °C were immersed in 5 mM N_3 dye (Ru (dcbpy)$_2$(NCS)$_2$ (dcbpy: 2,2′-bipyridine-4,4′-dicarboxylic acid) absolute ethanol solution for 24 h to complete the dye sensitizing. The dye-sensitized working electrodes and the platinized CEs were assembled to form sandwich-type DSCs by filling with a liquid electrolyte, which was composed of 0.5 M LiI, 0.02 M I_2, 0.3 M 1-methyl-3-hexylimidazolium iodide, and 0.5 M 4-*tert*-butylpyridine in 3-methoxypropionitrile, in the inner space between the two electrodes. The active area of the cells was 0.2 cm^2.

Characterization of the Platinized Electrodes and the DSCs. The surface morphology of the platinized electrodes was investigated by a scanning electron microscope equipped with an energy-dispersive X-ray analyzing system (SEM/EDX, Hitachi S-4800, 15 k V) and a high-resolution transmission electron microscope (TEM, JEM 2011, Japan; 200 kV). Optical transmittance spectra were recorded by a Hitachi U-3010 spectrophotometer. Platinum was dissolved off the platinized electrodes by aqua regia, and its content was determined by atomic emission spectroscopy with an axial view inductively coupled plasma spectrometer (SPECTRO Analytical Instruments GmbH). X-ray photoelectron spectroscopy analysis was carried out using a VG Scientific Escatab 220i-XL spectrometer with standard Al Kα radiation, and the working pressure is $<3 \times 10^{-9}$ mbar. Cyclic voltammograms (CVs) were performed on a Solartron SI 1287 electrochemical interface system at a scan rate of 100 mV s^{-1}. The electrolyte was an acetonitrile solution containing 10 mM LiI, 1 mM I_2, and 0.1 M $LiClO_4$. The electrochemical cell consisted of the platinized electrode as working electrode, a Pt wire as counter electrode, and an Ag/AgCl as reference electrode. Electrochemical impedance spectroscopy was used to obtain the charge transfer resistance (R_{ct}) data of the platinized electrodes. The measurements were performed on the DSCs under AM 1.5 illumination with a Solartron 1255B frequency response analyzer and a Solartron SI 1287 electrochemical interface system at open-circuit voltage. The frequency range was from 100 kHz down to 0.1 Hz, and the amplitude of the ac voltage was 10 mV. The photocurrent−voltage performance of the DSCs was measured employing a computer-programmed Keithley 2611 SourceMeter under illumination with simulated sunlight (AM 1.5, 100 mW cm^{-2}) supplied by a solar simulator (Oriel, 91160-1000 91192, Perccell Technologies). The incident light was calibrated with a power meter (model 350) and a detector (model 262). The active area was 0.2 cm^2.

Conflict of Interest: The authors declare no competing financial interest.

Acknowledgment. This work was financially supported by National Research Fund for Fundamental Key Project (2012CB932903), Foundation of Chinese Academy of Sciences (KGCX2-YW-386-2), and Nation Natural Science Foundation of China (20973183).

Supporting Information Available: XPS spectra of the obtained Pt electrode, schematic representation of the adhesive tape test, SEM images of the platinized electrodes before and after the adhesive tape test, and stability evaluation of the DSC are presented. This material is available free of charge *via* the Internet at http://pubs.acs.org.

REFERENCES AND NOTES

1. O'Regan, B.; Grätzel, M. A Low-Cost, High-Efficiency Solar Cells Based on Dye-Sensitized Colloidal TiO_2 Films. *Nature* **1991**, *353*, 737–740.
2. Yella, A.; Lee, H. W.; Tsao, H. N.; Yi, C.; Chandiran, A. K.; Nazeeruddin, M. K.; Diau, E. W. G.; Yeh, C. Y.; Zakeeruddin, S. M.; Grätzel, M. Porphyrin-Sensitized Solar Cells with Cobalt (II/III)-Based Redox Electrolyte Exceed 12% Efficiency. *Science* **2011**, *334*, 629–634.
3. Chen, D. H.; Huang, F. Z.; Cheng, Y. B.; Cruso, R. A. Mesoporous Anatase TiO_2 Beads with High Surface Areas and Controllable Pore Sizes: A Superior Candidate for High-Performance Dye-Sensitized Solar Cells. *Adv. Mater.* **2009**, *21*, 2206–2210.
4. Lindström, H.; Holmberg, A.; Magnusson, E.; Lindquist, S. E.; Malmqvist, L.; Hagfeldt, A. A New Method for Manufacturing Nanostructured Electrodes on Plastic Substrates. *Nano Lett.* **2001**, *1*, 97–100.
5. Ito, S.; Ha, N. L. C.; Rothenberger, G.; Liska, P.; Comte, P.; Zakeeruddin, S. M.; Péchy, P.; Nazeeruddin, M. K.; Grätzel, M. High-Efficiency (7.2%) Flexible Dye-Sensitized Solar Cells with Ti-Metal Substrate for Nanocrystalline-TiO_2 Photoanode. *Chem. Commun.* **2006**, *38*, 4004–4006.
6. Fu, N. Q.; Xiao, X. R.; Zhou, X. W.; Zhang, J. B.; Lin, Y. Electrodeposition of Platinum on Plastic Substrates as Counter Electrodes for Flexible Dye-Sensitized Solar Cells. *J. Phys. Chem. C* **2012**, *116*, 2850–2857.
7. Park, J. H.; Jun, Y.; Yun, H. G.; Lee, S. Y.; Kang, M. G. Fabrication of an Efficient Dye-Sensitized Solar Cell with Stainless Steel Substrate. *J. Electrochem. Soc.* **2008**, *155*, F145–F149.
8. Kim, D.; Ghicov, A.; Albu, S. P.; Schmuki, P. Bamboo-Type TiO_2 Nanotubes: Improved Conversion Efficiency in Dye-Sensitized Solar Cells. *J. Am. Chem. Soc.* **2008**, *130*, 16454–16455.
9. Yamaguchi, T.; Tobe, N.; Matsumoto, D.; Nagai, T.; Arakawa, H. Highly Efficient Plastic-Substrate Dye-Sensitized Solar Cells with Validated Conversion Efficiency of 7.6%. *Sol. Energy Mater. Sol. Cells* **2010**, *94*, 812–816.
10. Hauch, A.; Georg, A. Diffusion in the Electrolyte and Charge-transfer Reaction at the Platinum Electrode in Dye-Sensitized Solar Cells. *Electrochim. Acta* **2001**, *46*, 3457–3466.
11. Ramasamy, E.; Lee, J. Large-Pore Sized Mmesoporous Carbon Electrocatalyst for Efficient Dye-Sensitized Solar Cells. *Chem. Commun.* **2010**, *46*, 2136–2138.
12. Chen, J. K.; Li, K. X.; Luo, Y. H.; Guo, X. Z.; Li, D. M.; Deng, M. H.; Huang, S. Q.; Meng, Q. B. A Flexible Carbon Counter Electrode for Dye-Sensitized Solar Cells. *Carbon* **2009**, *47*, 2704–2708.
13. Wu, M. X.; Lin, X.; Wang, T. H.; Qiu, J. S.; Ma, T. L. Low-Cost Dye-Sensitized Solar Cell Based on Nine Kinds of Carbon Counter Electrodes. *Energy Environ. Sci.* **2011**, *4*, 2308–2315.
14. Roy-Mayhew, J. D.; Bozym, D. J.; Punckt, C.; Aksay, I. A. Functionalized Graphene as a Catalytic Counter Electrode in Dye-Sensitized Solar Cells. *ACS Nano* **2010**, *4*, 6203–6211.
15. Pringle, J. M.; Armel, V.; MacFarlane, D. R. Electrodeposited PEDOT-on-Plastic Cathodes for Dye-Sensitized Solar Cells. *Chem. Commun.* **2010**, *46*, 5367–5369.
16. Tai, Q. D.; Chen, B. L.; Guo, F.; Xu, S.; Hu, H.; Sebo, B.; Zhao, X. Z. *In Situ* Prepared Transparent Polyaniline Electrode and Its Application in Bifacial Dye-Sensitized Solar Cells. *ACS Nano* **2011**, *5*, 3795–3799.
17. Wang, M. K.; Anghel, A. M.; Marsan, B.; Ha, N. L. C.; Pootrakulchote, N.; Zakeeruddin, S. M.; Grätzel, M. CoS Supersedes Pt as Efficient Electrocatalyst for Triiodide Reduction in Dye-Sensitized Solar Cell. *J. Am. Chem. Soc.* **2009**, *131*, 15976–15977.
18. Li, G. R.; Wang, F.; Jiang, Q. W.; Gao, X. P.; Shen, P. W. Carbon Nanotubes with Titanium Nitride as A Low-Cost Counter-Electrode Material for Dye-Sensitized Solar Cells. *Angew. Chem., Int. Ed.* **2010**, *49*, 3653–3656.
19. Wu, M. X.; Lin, X.; Hagfeldt, A.; Ma, T. L. A Novel Catalyst of WO_2 Nanorod for the Counter Electrode of Dye-Sensitized Solar Cells. *Chem. Commun.* **2011**, *47*, 4535–4537.
20. Ito, S.; Zakeeruddin, S. M.; Comte, P.; Liska, P.; Kuang, D.; Grätzel, M. Bifacial Dye-Sensitized Solar Cells Based on an Ionic Liquid Electrolyte. *Nat. Photonics* **2008**, *2*, 693–698.
21. Peng, S. J.; Liang, J.; Mhaisalkar, S. G.; Ramakrishna, S. *In Situ* Synthesis of Platinum/Polyaniline Composite Counter Electrodes for Flexible Dye-Sensitized Solar Cells. *J. Mater. Chem.* **2012**, *22*, 5308–5311.
22. Kalyanasundaram, K. *Dye Sensitized Solar Cells*; EPFL Press & CRC Press: Lausanne, Switzerland, 2010.
23. Kavan, L.; Yum, J. H.; Grätzel, M. Optically Transparent Cathode for Dye-Sensitized Solar Cells Based on Graphene Nanoplatelets. *ACS Nano* **2011**, *5*, 165–172.
24. Papageorgiou, N.; Maier, W. F.; Grätzel, M. An Iodine/Triiodide Reduction Electrocatalyst for Aqueous and Organic Media. *J. Electrochem. Soc.* **1997**, *144*, 876–884.
25. Liang, H. W.; Cao, X.; Zhou, F.; Cui, C. H.; Zhang, W. J.; Yu, S. H. A Free-Standing Pt-Nanowire Membrane as a Highly Stable Electrocatalyst for the Oxygen Reduction Reaction. *Adv. Mater.* **2011**, *23*, 1467–1471.
26. Lee, Y. L.; Chen, C. L.; Chong, L. W.; Chen, C. H.; Liu, Y. F.; Chi, C. F. A Platinum Counter Electrode with High Electrochemical Activity and High Transparency for Dye-Sensitized Solar Cells. *Electrochem. Commun.* **2010**, *12*, 1662–1665.
27. Sun, K.; Fan, B. H.; Ouyang, J. Y. Nanostructured Platinum Films Deposited by Polyol Reduction of a Platinum Precursor and Their Application as Counter Electrode of Dye-Sensitized Solar Cells. *J. Phys. Chem. C* **2010**, *114*, 4237–4244.
28. Chen, L. L.; Tan, W. W.; Zhang, J. B.; Zhou, X. W.; Zhang, X. L.; Lin, Y. Fabrication of High Performance Pt Counter Electrodes on Conductive Plastic Substrate for Flexible Dye-Sensitized Solar Cells. *Electrochim. Acta* **2010**, *55*, 3721–3726.
29. Kim, S. S.; Nah, Y. C.; Noh, Y. Y.; Jo, J.; Kim, D. Y. Electrodeposited Pt for Cost-Efficient and Flexible Dye-Sensitized Solar Cells. *Electrochim. Acta* **2006**, *51*, 3814–3819.
30. Yin, X.; Xue, Z. S.; Liu, B. Electrophoretic Deposition of Pt Nanoparticles on Plastic Substrates as Counter Electrode for Flexible Dye-Sensitized Solar Cells. *J. Power Sources* **2011**, *196*, 2422–2426.
31. Lee, J.; Choi, W. Effect of Platinum Deposits on TiO_2 on the Anoxic Photocatalytic Degradation Pathways of Alkylamines in Water: Dealkylation and N-Alkylation. *Environ. Sci. Technol.* **2004**, *38*, 4026–4033.
32. He, C.; Xiong, Y.; Zhu, X. H.; Li, X. Z. A Platinised TiO_2 Film with Both Photocatalytic and Non-Photocatalytic Activities towards the Oxidation of Formic Acid. *Appl. Catal., A* **2004**, *275*, 55–60.
33. Yamakata, A.; Ishibashi, T.; Onishi, H. Water-and Oxygen-Induced Decay Kinetics of Photogenerated Electrons in TiO_2 and Pt/TiO_2: A Time-Resolved Infrared Absorption Study. *J. Phys. Chem. B* **2001**, *105*, 7258–7262.
34. Tan, W. W.; Chen, J. M.; Zhou, X. W.; Zhang, J. B.; Lin, Y.; Li, X. P.; Xiao, X. R. Preparation of Nanocrystalline TiO_2 Thin Film at Low Temperature and Its Application in Dye-Sensitized Solar Cells. *J. Solid State Electrochem.* **2009**, *13*, 651–656.
35. Lee, H.; Hwang, D.; Jo, S. M.; Kim, D.; Seo, Y.; Kim, D. Y. Low-Temperature Fabrication of TiO_2 Electrodes for Flexible Dye-Sensitized Solar Cells Using an Electrospray Process. *ACS Appl. Mater. Interfaces* **2012**, *4*, 3308–3315.
36. Alam, M. J.; Cameron, D. C. Optical and Electrical Properties of Transparent Conductive ITO Thin Films Deposited by Sol-Gel Process. *Thin Solid Films* **2000**, *377*, 455–459.
37. Teranishi, T.; Hosoe, M.; Tanaka, T.; Miyake, M. Size Control of Monodispersed Pt Nanoparticles and Their 2D Organization by Electrophoretic Deposition. *J. Phys. Chem. B* **1999**, *103*, 3818–3827.
38. Kim, Y. J.; Lee, Y. H.; Lee, M. H.; Kim, H. J.; Pan, J. H.; Lim, G. I.; Choi, Y. S.; Kim, K.; Park, N. G.; Lee, W. I. Formation of Efficient Dye-Sensitized Solar Cells by Introducing an Interfacial Layer of Long-Range Ordered Mesoporous TiO_2 Thin Film. *Langmuir* **2008**, *24*, 13225–13230.
39. Yoo, B.; Kim, K.; Lee, D. K.; Ko, M. J.; Lee, H.; Kim, Y. H.; Kim, W. M.; Park, N. G. Enhanced Charge Collection Efficiency by

Thin-TiO_2-Film Deposition on FTO-Coated ITO Conductive Oxide in Dye-Sensitized Solar Cells. *J. Mater. Chem.* **2010**, *20*, 4392–4398.
40. Bard, A. J. *Electrochemical Methods: Fundamentals and Applications*; Faulkner, L. R., Ed.; Wiley: New York, 2001; pp 8−9.
41. Lin, L. Y.; Nien, P. C.; Lee, C. P.; Tsai, K. W.; Yeh, M. H.; Vittal, R.; Ho, K. C. Low-Temperature Flexible Photoanode and Net-Like Pt Counter Electrode for Improving the Performance of Dye-Sensitized Solar Cells. *J. Phys. Chem. C* **2010**, *114*, 21808–21815.
42. Snaith, H. J.; Schmidt-Mende, L.; Grätzel, M. Light Intensity, Temperature, and Thickness Dependence of the Open-Circuit Voltage in Solid-State Dye-Sensitized Solar Cells. *Phys. Rev. B* **2006**, *74*, 045306.